1. Introduction and Background

The Neoproterozoic Era is defined in geologic time from ~1,000 to ~541 million years ago. The Neoproterozoic is often characterized by researchers as a duration of the earth's history in which global systems dramatically shifted and conditions necessary for the emergence of more complex life became prevalent. This period of time underwent many critical events that contributed to defining present day earth. Notable events in this era include the assembly of the supercontinent Rodinia (Figure 1.) (marking the start of the Tonian period), along with the subsequent disassembly, and the last stages of the Great Oxygenation Event, during which atmospheric oxygen began accumulating in earnest and marked the start of the Cryogenian period (*Chandler and Sohl*, 2000). The most remarkable findings from the Neoproterozoic Era include the geologic and the paleomagnetic evidence that suggest multiple widespread glaciation events that extended to low latitudes, even reaching near equatorial latitudes at some

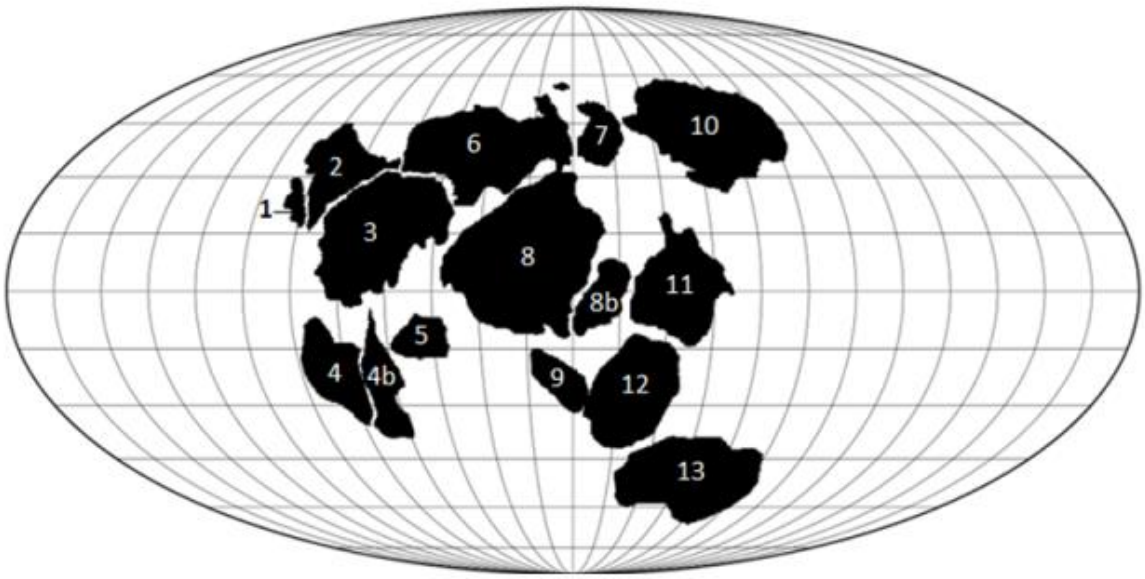

Figure 1. Mollweide map projection of the Rodinia paleocontinental configuration during the Sturtian Glacial Interval (~750Ma). Cratons are as follows: 1, Madagascar; 2, India; 3, East Antarctica; 4, 4b, Congo-Sao Francisco; 5, Kalahari; 6, Australia; 7, South China; 8, 8b, Laurentia; 9, Rio Plato; 10, Siberia; 11, Baltica; 12, Amazonia; 13, West Africa.

points (*Harland and Bidgood*, 1959; *Harland*, 1964; *Spencer*, 1971; *Li, et al.* 1995; *Fairchild, et al.*, 2018).

Kirschvink first termed the phrase Snowball Earth in his 1992 hypothesis. This hypothesis states that at some point in Earth's history, the globe underwent total glaciation, (*Harland*, 1964; *Kirschvink*, 1992). The Snowball Earth Hypothesis was proposed as a means to explain evidence of sea-level glacial deposits found at low paleolatitudes (*Harland and Bidgood*, 1959; *Harland*, 1964). The onset of the Sturtian glaciation (750-700 Ma) is thought to have been forced by the initial breakup of Rodinia, marked by when the Laurentia craton first began to separate near the center of the continent (*Gernon, et al.,* 2016). Formerly landlocked regions were then exposed to ocean moisture. This ocean moisture contributed to an enhanced mechanical weathering, which in turn strengthened chemical weathering. Atmospheric carbon dioxide is removed from the atmosphere via chemical (silicate) weathering, which resulted in a rapid drop in temperature. Declining temperatures helped generate an insuppressible cooling effect which engulfed the entire planet. This process has been termed as a runaway ice albedo feedback loop (*Hoffman and Schrag*, 2000). Others who have investigated this event have suggested that the placement of the primary land mass, Rodinia, in low latitudes is a vital step in inducing the feedback loop with the potential to bring global glaciation. Ice coverage in high latitudes prevents chemical erosion of rocks beneath the surface and suppresses the carbon burial process. Carbon dioxide in the atmosphere therefore prevents glacial ice sheets from advancing (*Schrag, et al.,* 2002). But since land masses concentrated in the low latitudes rather than high,

chemical erosion was not stifled and the threshold for a runaway freezing episode was soon reached (*Hoffman and Schrag,* 2000). Snow and ice, having high albedos, reflected warm solar insolation from the continents and oceans back into space. Their albedo effect and increase in surface area induced a continuous cycle of global cooling. If ice extent ever reached 50% of the surface area of the planet, it is believed that the feedback would become self-sustaining (*Schrag, et al.,* 2002*)*. The Snowball Earth Hypothesis claimed that the earth did in fact reach the 50% threshold necessary to allow for ice to extend all the way to the equator (*Kirschvink*, 1992; *Hoffman, et al.,* 1998; *Hoffman and Schrag*, 2000).

There are issues with the Snowball Earth Hypothesis, however. One major aspect that was slightly overlooked and needed further exploring was a mechanism for deglaciation. As stated in *Hoffman, et al.* (1998), the cooling feedback would become self-sustaining should the majority of the earth's surface undergo glaciation. In order to reverse the work done by the cooling feedback loop, the Earth would require massive amounts of radiative input in order to facilitate its escape from the feedback loop (*Crowley, et al.,* 2001). This deglaciation conundrum is evaded, though, if the planet never reached a full Snowball state in the first place where ice reached the equator. A Waterbelt (*Pierrehumbert, et al.,* 2011) state has been proposed to counter the idea of equatorial glaciation and elaborates that a band of water existed encompassing the equator. This Waterbelt state is favored by current studies and researchers for two reasons: (1) even with the most up to date Rodinia continental configuration and extremely low levels of atmospheric CO2, a solid Snowball state is

extremely difficult to induce in models without setting an unrealistically low solar luminosity *(Crowley and Baum*, 1993; *Chandler and Sohl*, 2000; *Tziperman, et al.*, 2012) and (2) there is a lack of evidence that a major extinction event occurred. If total glaciation occurred, then the oceans would be completely sealed and there would be evidence for a widespread elimination of photosynthetic plankton in the stratigraphic record *(Tziperman, et al.,* 2012; *Rose*, 2015).

There are two primary goals for this paper. The first goal is to determine whether CO2 levels or solar luminosity have a greater effect on glacial dynamics. Secondly, this paper strives to determine what basic forcings might be necessary to induce total glaciation.

2. METHODS

2.1. The Model

EdGCM (*Chandler, et al.*, 2005) is a general circulation model based on the Goddard Institute for Space Studies general circulation model (*Hansen, et al.,* 1983; *Chandler and Sohl*, 2000), but is modified for academic purposes. It is a three dimensional model which solves numerically the physical conservation equations for mass, energy, momentum, and moisture, along with equation of state for 8˚x10˚ grid spaces that extend nine layers in the atmosphere. A parsed earth allows for calculations to be made on specific regions and helps the user identify specific areas of interest. Both a seasonal and a 24-hour diurnal solar cycles are factored in to make temperature calculations. Snow accumulation accounts for the combination of snowfall, melting, and sublimation. Ocean heat convergences account for seasonal and regional variances in climate. Surface energy fluxes are model

derived values; both the ocean heat convergences and the surface energy fluxes are used to calculate sea surface temperatures.

The GCM uses five harmonics when defining a seasonally varied energy flux and upper ocean energy storage to facilitate more accurate approximations in regions of sea ice formation. Sea ice forms via solely thermodynamic mechanisms with no influence from wind stress or ocean dynamics. When a grid cell reaches -1.6˚, a block of ice 0.5m thick will form over a fraction of the cell. This ice will respond as needed to maintain energy balance; this includes growing or shrinking both vertically and horizontally. Ice will begin to melt when a grid cell warms to 0˚C. There is a simulated ice/albedo feedback that is relevant to this study as it would alter sea ice and snow cover and is fully explained in *Hansen, et al.* (1983). Essentially, the albedo of snow is a function of age and depth, with fresh snow maintaining an albedo of 0.85 for 50 days and changes to 0.5 after 50 days. The albedo of snow-free sea ice is set to 0.3 in the near infrared and 0.55 in the visible and is independent of age and thickness.

2.2.Forcings

This study aims to determine the dependency of glaciation on luminosity

Table 1. Values for Altered Forcings

Run Label	CO2 Concentration (ppm)	Solar Reduction (%)
A	120	4
B	140	6
C	160	8
D	120	4
E	140	6
F	160	8
G	120	4
H	140	6
I	160	8

Forcings that were altered for each simulation are shown; other forcings remain the same as Run A. All simulations use the Sturtian paleocontinental reconstruction (see Figure 1.) as a land surface boundary condition

versus atmospheric carbon dioxide concentrations. Nine trials ran using the Rodinia configuration (Figure 1.) as the boundary conditions. Rodinia was given a uniform desert condition with no plants present, as vascular vegetation is undeveloped at this time (*Chandler and Sohl*, 2000). The trials ran using a combination of varied CO2 concentrations and lowered solar luminosity, as listed in Table 1. Orbital forcings were based on modern conditions, with obliquity set to 23.44˚, eccentricity set to 0.0167, and omegaT (precession) set to 282.9˚. Additionally, Earth's rotation rate was set to the modern rate of 24-hours per 1 rotation, rather than an increased 18-hour rotation period that would have been seen in the Neoproterozoic (Hyde *et al.*, 2000).

We hypothesized that despite drastic reductions in both solar luminosity and CO2 concentrations, EdGCM would not be able to model a total glaciation without updated ocean dynamics and the feature to model ice sheets. We also hypothesized that solar luminosity would have a greater effect on the extent of sea ice and snow coverage.

3. RESULTS

All of the simulation ran long enough for the earth's climate to reach an equilibrium point, which varied from trial to trial, but generally occurred at or around 50 years. After equilibrium was established, the model continued to run each simulation for approximately 10 years, after which the physics of the system failed. Some of the runs (A, B, and C) ran nearly to completion, while other runs failed after only 60 years. This will be further discussed in section 4.1.

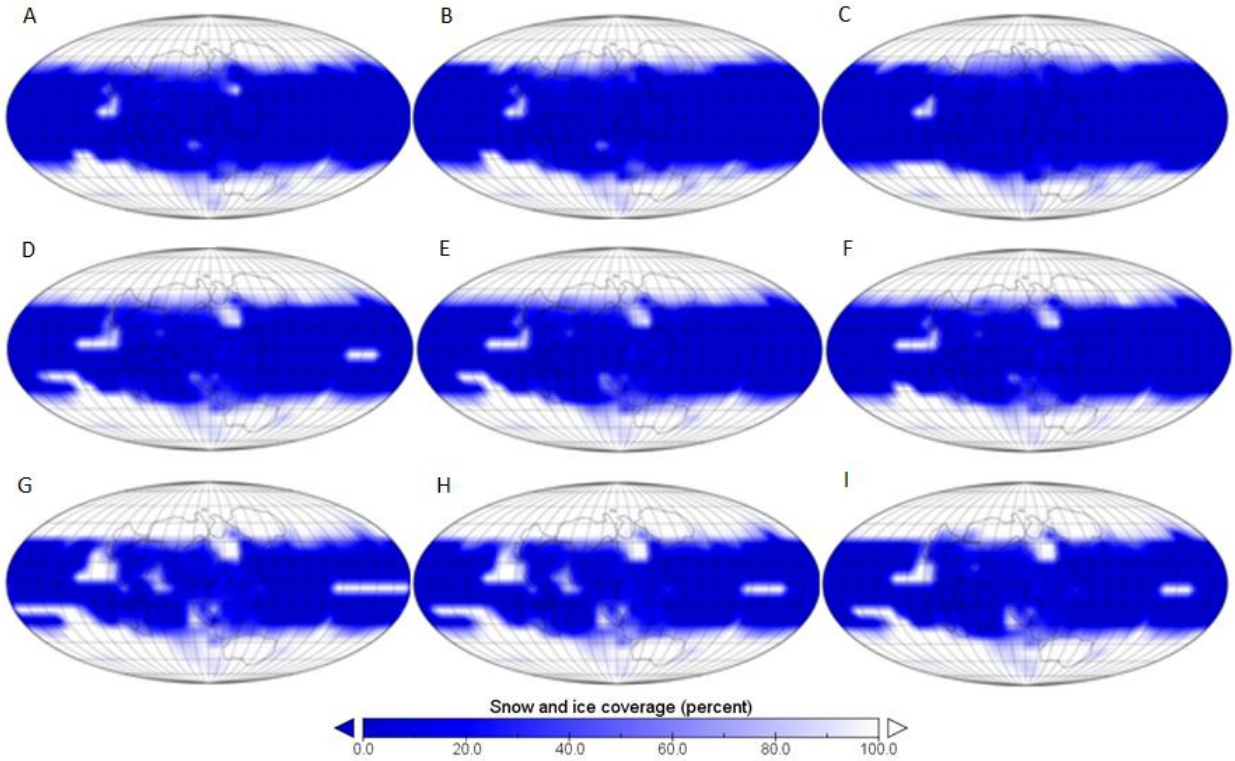

Figure 2. Snow and ice coverage. Individual maps are labeled according to the run label. All simulations use the Sturtian paleocontinental reconstruction (Figure 1.).

3.1. Snow and Ice Cover

Run C proved to be the warmest of all nine trials, with an annual average of 38.1% snow and ice cover. Coverage did not extend past 32° latitude. Runs D, E, and F had an average combined snow and ice surface coverage of 45.8%. Of these three runs, snow and ice coverage in run D spread to the lowest latitudes, reaching 31° latitude in both the northern and southern hemispheres. Each hemisphere also showed ice tongues that approached nearly 25° latitude, but no further. Runs G, H, and I resulted in the earth's coldest conditions with an average combined snow and ice coverage of 52.23%. Runs G and H surpassed the 50% snow and ice coverage marker, while run I was fairly close. The run nearly reached the critical 50% coverage required to launch a self-sustaining feedback loop. Run I displayed an average snow and ice coverage of 49.6%. Run G

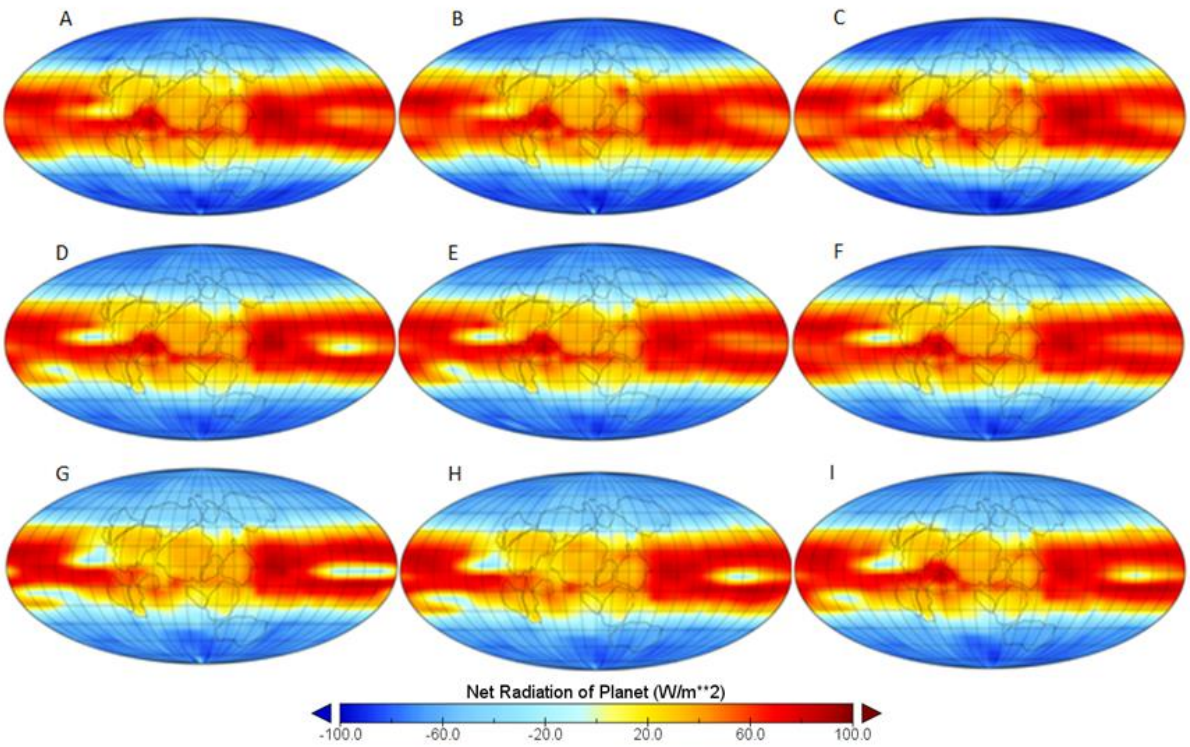

Figure 3. Annual net radiation (see Figure 2 for legend).

proved to be the coldest run with snow and ice coverage reaching to nearly 28° latitude. This run also experienced cold tongues that extended down to 25° latitude.

3.2. Annual Net Radiation

The net radiation for all nine runs nearly approached zero. Only runs B and C displayed positive net radiations which ended up being valued at 0.3 W/m2 and 0.5 W/m2 respectively. The other seven remaining runs experienced an average net global cooling effect. Run G generated the strongest net radiative cooling at -3.0 W/m2.

3.3. Annual Sea Surface Temperatures

Sea surface temperatures were reasonable and correlate with the results for snow and ice coverage and net radiation. The warmest temperatures occur near the equator and progressively get colder toward the poles. In the warmest scenario (C), the mean sea surface

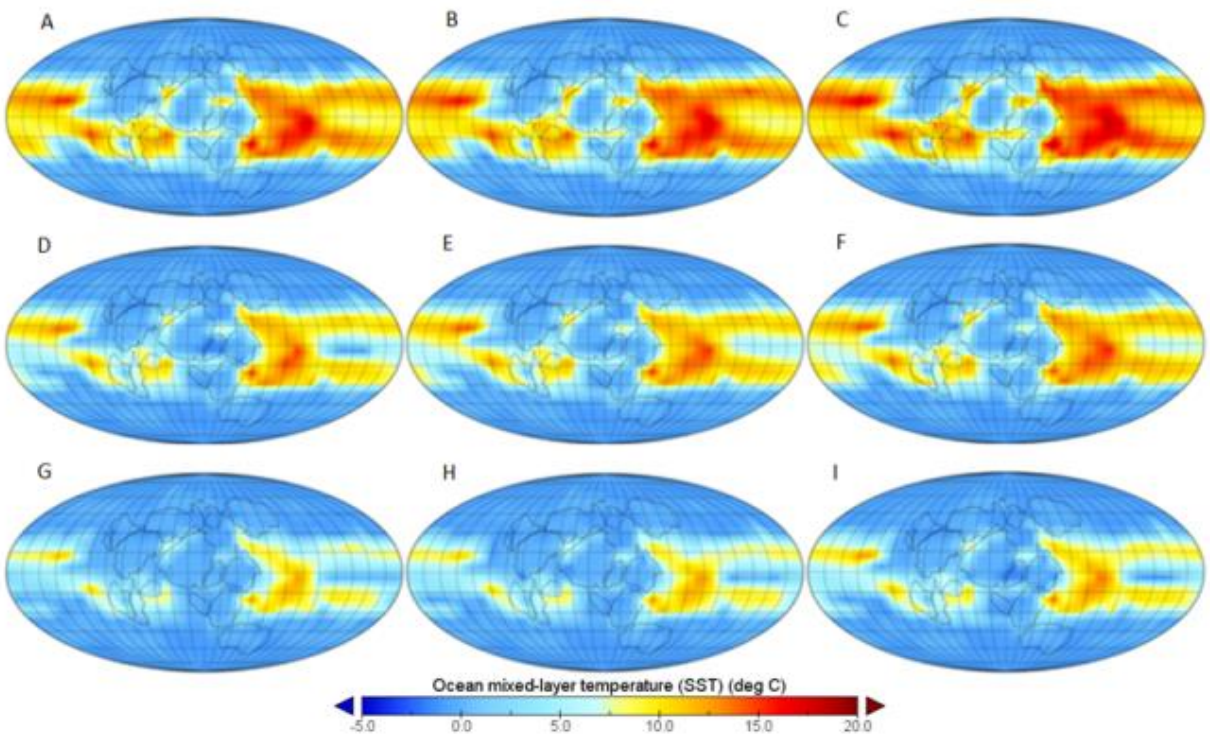

Figure 4. Annual sea surface temperatures (see Figure 2 for legend).

temperature was 5.1°C. This run had a belt of much warmer water in the low latitudes, with a maximum of 18°C. The equator to pole gradient in the coldest scenario (G) is almost nonexistent, with the majority of the oceans residing at 1.8°C and isolated areas near the equator reaching only 13.2°C.

3.4. Cloud Cover

The distribution of clouds varies by both cloud height and latitude (see Figure 4a). Coverage by high clouds in both runs lingers at around 20% in the mid-latitudes, and rises to around 30% in the tropics. High cloud cover is zero at the poles. Coverage by low clouds reveals more latitudinal variance, reaching up to 80% coverage in the poles, 50-60% in the mid-latitudes, and dropping to about 30% in the tropics.

4. Discussion

4.1. Errors and Anomalies

As reported above, each run reached equilibrium, but none were able to run the

simulation to completion. Since EdGCM works mainly using calculations of moisture, mass, energy, and momentum, if one or more of these calculations is unable to compute to completion, the physics of the system fails and the run stops. The simulation is unable to create ice sheets, but is capable of modelling sea ice formation as described in our methods. However, since the simulation uses a mixed-layer ocean model, it is possible that extreme conditions, such as those seen in our simulations, could cause one or more grid cells to freeze solid through the bottom of the layer. The result of grids freezing repeatedly this may ruin the simulation. When this occurs repeatedly, the result is a disruption of the calculations needed to continue running the simulation, and thus the run is terminated at this point (M. Chandler, personal communication, October 10, 2016; M.Chandler, personal communication, November 15, 2018). Because none of the runs ended at the same time, data from years 55-60 were used to create plots from all runs.

Review of the snow and ice cover revealed more doubt in the EdGCM results. Simulations revealed isolated regions of ice formation near the equator off the coasts of the East Antarctic craton and Baltica. These equatorial glaciations are present in each run, despite forcings that would strongly hinder ice growth at these latitudes. Furthermore, the extent of this anomalous glaciated region does not change from run to run (within runs of the same solar forcings). This piece of evidence was therefore written off as error in the simulation's calculations. This error is also present in net radiation, sea surface temperatures, and cloud cover plots, and is also disregarded. After dismissing this data as credible evidence, the simulations show

even more clearly the extents of climate variances during the period of glaciation.

4.2. Response of Snow and Ice Cover to Forcings

Snow and ice cover varied little from each of the trials within the runs of the same solar forcings; i.e. snow and ice accumulation seems to vary more between trials with the same CO2 forcings and varying luminosity. A 1.8 and 2.1% difference in total snow and ice cover exists between runs A-B and B-C, respectively; 1.4 and 1.1% difference in cover from D-E and E-F, respectively; and 1.5 and 3.2% difference in cover from G-H and H-I, respectively. Differences in ice and snow cover between runs A-D-G, B-E-H, and C-F-I, however, lay between 5 and 7%.

None of the simulations produced results with snow and ice cover in the tropics for any extended period of time, leaving a belt of water around the equator. This aligns with similar studies (*Crowley, et al.*,1993; *Jenkins, et al.*, 1998; *Chandler and Sohl*, 2000; *Rose*, 2015).

4.3. Response of Sea Surface Temperature to Forcings

Annual sea surface temperatures varied analogously to the variations in snow and ice coverage, with more difference between runs of different solar forcings and less difference seen in runs with different CO2 forcings. There's regionally warmer water surrounding the equator (-30˚ to 30˚), with average temperatures of this region ranging from about 5˚C to 13.2˚C in run G and 18.8˚C in run C. The higher sea surface temperatures of this region. The differences in temperatures contributed to the lack of snow and ice cover.

4.4. Response of Net Planetary Radiation to Forcing

Orbital forcings were not adjusted for these simulations, though there is some

suggestion that orbital periods may have been ~20% shorter (*Crowley and Baum,* 1993). We cannot accurately incorporate these suggestions into models because we do not know the difference in magnitude of the forcings during the time period of interest from the current magnitude. Orbital forcings were unchanged from current states, thus the distribution of radiation was similar to current distribution of radiation, with a deficit over the poles and surplus over the equator. Comparison of net planetary radiation from both runs C and G, as well as present-day net planetary radiation measurements suggests that latitudinal variability in net radiation increases as luminosity increases (Figure 5A).

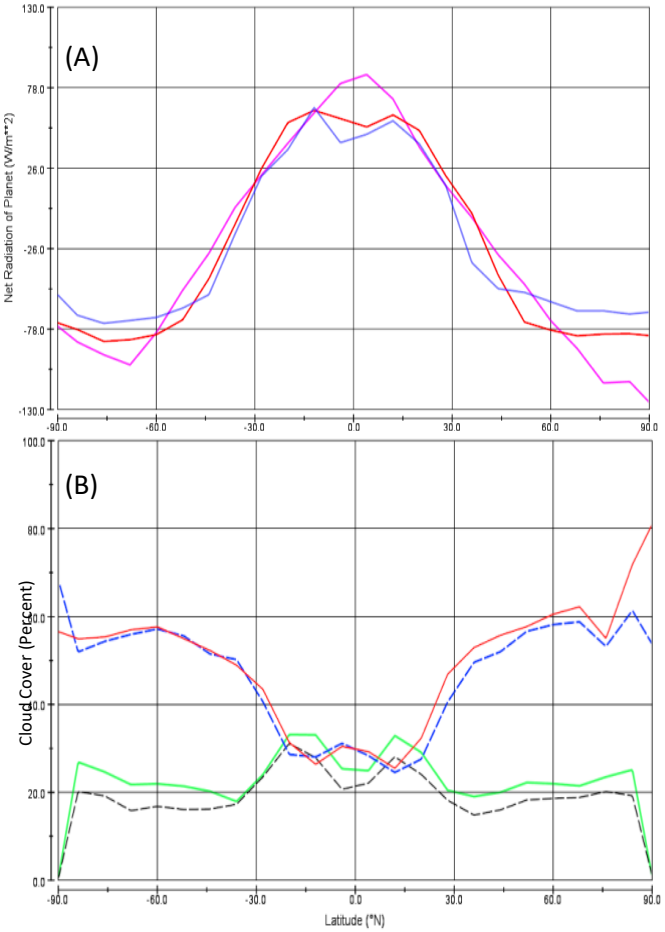

Figure 5. (A) Annual net planetary radiation from runs C (blue), G (red), and modern measurements (pink). (B) High and low cloud coverage from run C (green and blue dashed, respectively) and from run G (black dashed and red, respectively).

4.5. Response of Cloud Cover to Forcings

Cloud cover may have been both an influence and result of net planetary radiation. High clouds generally have a warming effect and a lower water content, while low clouds tend to have a cooling effect and higher water content (*Pierrehumbert, et al.*, 2005; *Abbot, et al.*, 2012). The cooling and warming effects align with the distribution of net radiation seen in the simulations (Figure 5). The

tropics receive the most coverage from high clouds seen anywhere in the simulation, while also seeing the scarcest coverage from low clouds. Clouds in the tropics are thus believed to have a slight warming effect that affects net radiation and extent of snow and ice cover.

4.6. Comparison to the Literature

Our results closely resemble those of previous modelling experiments performed to look at different regions and times of glaciation periods on earth (*Crowley and Baum*, 1993; *Jenkins and Frakes*, 1998; *Chandler and Sohl*, 2000).

Crowley and Baum (1993) initially used a simple southern hemisphere continent consistent with the basic Pannotia/Varanger configuration (Figure 6, taken from *Chandler and Sohl*, 2000) to model the Varanger glaciation (~610-575 Ma), and secondly used a simple rectangular continent in the low latitudes to simulate the Sturtian glaciation. Their second model's results showed that glaciation could initiate on a horizontally oriented low latitude continent with CO2 levels at 120 ppm, but requires a 20% reduction in solar luminosity. The 20% reductions are unrealistic conditions for earth to sustain when interpreting the solar luminosity curve (Figure 7, from *Crowley and Baum*, 1993). The simulation also showed that a positive snow and ice albedo feedback loop can be induced over a region with permanent snow, which can influence and encourage mid-to-high latitude glaciation. *Crowley and Baum* (1993) satisfied many pieces of evidence for low latitude glaciation, but were unable to

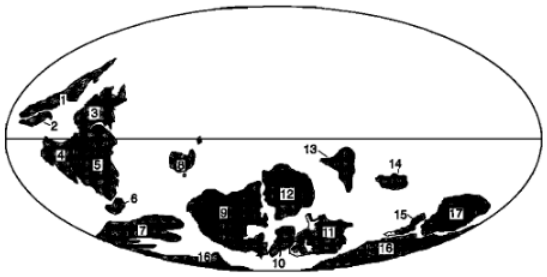

Figure 6. Pannotia/Varanger configuration (Chandler and Sohl, 2000)

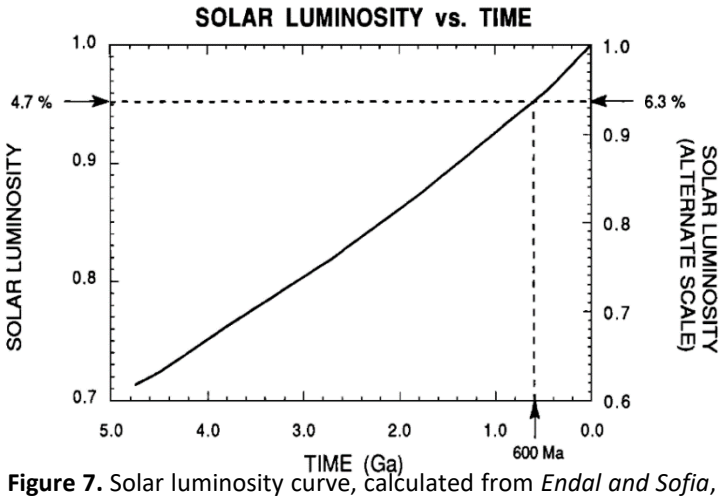

Figure 7. Solar luminosity curve, calculated from *Endal and Sofia*, 1981.

reveal a mechanism for sea-level equatorial glaciation (*Crowley and Baum*, 1993).

Jenkins and Frakes (1998) used the GENESIS R15 model (developed by *Johnson and Pollard,* 1995) with a horizontal resolution of 4.5˚x7.5˚, to run a series of simulations with forcings similar the ones used in our study. Additional boundary parameters were included in this case. GENESIS ran with a simple horizontally oriented rectangular continent, centered on the equator that included a mountain range running north-to-south across the face of the continent. The results of the simulations showed that it is difficult to produce conditions favorable for low-latitude glaciation. Similar to *Crowley and Baum* (1993), the GENESIS simulations showed that initiation of global glaciation occurs over land where permanent snow occurs. *Jenkins and Frakes* also observe, however, that arid conditions combined with cloud cover at less than 20 percent over the interior of the continent inhibits the possibility of equatorial glaciation. *Jenkins and Frakes* thus argue that incident solar radiation at the surface must decrease and precipitation rates must increase to accommodate for the conditions necessary to form a total global glaciation (*Jenkins and Frakes*, 1998).

Chandler and Sohl (2000) use the GISS GCM model that is the base model of EdGCM. Their study, however, focused on the Varanger glaciation rather than the Sturtian glaciation and the only parameter changed from the ones used in this study (in

the runs that are analogous to ours) was the continental configuration (Figure 6). Though the continental boundaries were shifted, the GCM was unable to produce a 'hardball' state where the entire globe was covered in ice. The results of their simulations produced cloud cover that was similar in value to that observed in this study, though the distribution was shifted due to their boundary conditions (*Chandler and Sohl*, 2000).

5. Conclusion

The EdGCM model was designed as a way for students to explore climate variables and dynamics. For this purpose, the model is enough in its calculations and calibrations that would be relevant for academic purposes. With EdGCM, we were able to simulate various scenarios with mixed forcings to suggest that the climate system is more sensitive to changes in solar luminosity than to changes in atmospheric CO2 concentrations. From this conclusion, we also suggest that further trials should be run at 6% reduction in solar luminosity with decreasing amounts of CO2 as an attempt to induce total glaciation.

However, there are certain parameters that are vital to the investigation of climate states, past and present, that are absent from the model, but must be addressed. These include, but are not limited to, ice sheet dynamics, cloud mechanics and feedbacks, ice-albedo feedbacks, orbital and diurnal variations, and seasonal changes in convection cells. Efforts have been made over the past few years to provide more accurate models, but given the complexity of the climate system, progress has been slow. Major steps have been taken, however, in experimenting with different glaciation and deglaciation mechanisms. *Abbot et al.* (2010), *Abbot, et al.* (2012), and *Abbot* (2014) are a series of

papers that investigate and make significant headway on quantifying cloud radiative forcing and deglaciation thresholds. CO2 forcings are difficult to model, as one must account for the neutralization of the carbonate reservoir (*Crowley et al.,* 2001, *Pierrehumbert*, 2011), which, of course, leads to the need to account for the approximate size of the carbonate reservoir. Though, *Abbot* (2010, 2013, and 2014) has made significant headway in this topic, there are more factors that must be investigated.

Progress has been made in the reconstruction of the paleogeography. *Arnaud* (2004) performed sedimentological analysis of the Port Askaig Formation, a formation that is part of a Supergroup that is thought to record the rifting of Rodinia as well as containing 'cap' carbonates that are characteristic of the rapid Sturtian deglaciation. The critical piece of evidence from this study is the assessment of cross-bedding in the sandstone member of this formation. Analysis highly suggests that this cross bedding formed via tidal currents, i.e. the ocean was not sealed during the Sturtian glaciation (*Arnaud*, 2004).

Furthermore, strides have been made in the field of paleomagnetism, which help to further parameterize the boundary conditions of the Rodinia continental configuration (*Tziperman, et al.*, 2012; *Fairchild, et al.*, 2018; *Zhao, et al.*, 2018; *Campanha, et al.*, 2019).

And lastly, there have been contributions to the field of paleoceanography, which further add to the list of parameterizations that our models are built upon. *Ashkenazy, et al.* (2013), among several others, has taken initial steps in simulating the dynamics of a Snowball Earth ocean. Their initial model failed to include chemically driven density differences. *Gernon, et al.*

(2015) uses Monte Carlo simulations to demonstrate how enhanced volcanism due to the Rodinia break up contributes to an alkaline shift in ocean chemistry before and during the Sturtian glaciation. This, combined with paleogeographic data, will greatly help further our understanding of the ocean circulatory patterns. Developing a more complete understanding of the ocean process will be relevant in minding their impact on glaciation.

As a scientific community, we are moving toward a more complete understanding of climate dynamics and paleoclimate. Our knowledge of the climate dynamics and paleoclimate will allow for us to answer even bigger questions and better prepare for any future advancements. Future studies will hopefully be able to accurately incorporate this burgeoning information into new, more precise models. More accurate information will then be more reliable and more mainstreamed in everyday applications.

References

Abbot, D. S. (2014). Resolved Snowball Earth Clouds. https://doi.org/10.1175/JCLI-D-13-00738.1.

Abbot, D. S., & Pierrehumbert, R. T. (2010). Mudball: Surface dust and Snowball Earth deglaciation. *Journal of Geophysical Research*, *115*(D3), D03104. https://doi.org/10.1029/2009JD012007.

Abbot, D. S., Voigt, A., Branson, M., Pierrehumbert, R. T., Pollard, D., Le Hir, G., & Koll, D. D. B. (2012). Clouds and Snowball Earth deglaciation. *Geophysical Research Letters*, *39*(20). https://doi.org/10.1029/2012GL052861.

Arnaud, E. (2004). Giant cross-beds in the Neoproterozoic Port Askaig Formation, Scotland: implications for snowball Earth. *Sedimentary Geology*, *165*(1–2), 155–174. https://doi.org/10.1016/J.SEDGEO.2003.11.015.

Ashkenazy, Y., Gildor, H., Losch, M., Macdonald, F. A., Schrag, D. P., & Tziperman, E. (2013). Dynamics of a Snowball Earth ocean. *Nature*, *495*(7439), 90.

Campanha, G. A. C., Faleiros, F. M., Cawood, P. A., Cabrita, D. I. G.,

Ribeiro, B. V., & Basei, M. A. S. (2019). The Tonian Embu Complex in the Ribeira Belt (Brazil): revision, depositional age and setting in Rodinia and West Gondwana. *Precambrian Research*, *320*, 31–45. https://doi.org/10.1016/J.PRECAMRES.2018.10.010.

Chandler, M. A., & Sohl, L. E. (2000). *Climate forcings and the initiation of low-latitude ice sheets during the Neoproterozoic Varanger glacial interval*. *JOURNAL OF GEOPHYSICAL RESEARCH* (Vol. 105). https://doi.org/10.1029/2000JD900221.

Crowley, A. J., & Baum, S. K. (1993). *Effect of Decreased Solar Luminosity on Late Precambrian Ice Extent*. *JOURNAL OF GEOPHYSICAL RESEARCH* (Vol. 98). Moores. Retrieved from https://agupubs.onlinelibrary.wiley.com/doi/pdf/10.1029/93JD01415.

Endal, A. S., & Sofia, S. (1981). Rotation in Solar-Type Stars. I. Evolutionary Models for the Spin-Down of the Sun. *The Astrophysical Journal*, *243*, 6225–6640. Retrieved from http://adsbit.harvard.edu.

Fairchild, I. J., Hambrey|, M. J., & Jefferson^, T. H. (2018). Late Proterozoic glacial carbonates in northeast Spitsbergen: new insights into the carbonate–tillite association. *Geol. Mag*, *126*(5), 469–490. https://doi.org/10.1017/S0016756800022809.

Friedrich, T., Timmermann, A., Tigchelaar, M., Elison Timm, O., & Ganopolski, A. (2016). Nonlinear climate sensitivity and its implications for future greenhouse warming. *Science Advances*, *2*(11), e1501923. https://doi.org/10.1126/sciadv.1501923.

Gernon, T. M., Hincks, T. K., Tyrrell, T., Rohling, E. J., & Palmer, M. R. (2015). *Snowball Earth ocean chemistry driven by extensive ridge volcanism during Rodinia breakup*. Retrieved from https://eprints.soton.ac.uk/386413/1/snowball-NG-gernon-final.pdf.

Harland, W. B. (1964). Critical evidence for a great infra-Cambrian glaciation. *Geologische Rundschau*. https://doi.org/10.1007/BF01821169.

Harland, W.B., & Bidgood, D.E.T. (1959). Palæomagnetism in Some Norwegian Sparagmites and the Late Pre-Cambrian Ice Age. *Nature*, *184*(4702), 1860–1862. https://doi.org/10.1038/1841860b0.

Hoffman, P. F., & Schrag, D. P. (2002). The snowball Earth hypothesis: testing the limits of global change. *Terra Nova*, *14*(3), 129–155. https://doi.org/10.1046/j.1365-3121.2002.00408.x.

Hoffman, P. F., & Schrag, D. P. (2000). *Snowball Earth*. Retrieved from http://folk.ntnu.no/ystenes/div/bilder/sidesp/snow/snowball.pdf.

Jenkins, G. S., & Frakes, L. A. (1998). *GCM sensitivity test using increased rotation rate, reduced solar forcing and orography to examine low latitude glaciation in the Neoproterozoic* (Vol.

25). https://doi.org/10.1029/98GL52588.

Joseph L Kirschvink. (1992). *Late Proterozoic Low-Latitude Global Glaciation: the Snowball Earth*. New York. Retrieved from https://authors.library.caltech.edu/36446/1/Kirschvink_1992p51.pdf.

Lewis, J. P., Weaver, A. J., & Eby, M. (2006). Deglaciating the snowball Earth: Sensitivity to surface albedo. *Geophysical Research Letters*, *33*(23), L23604. https://doi.org/10.1029/2006GL027774.

Lewis, J. P., Weaver, A. J., Johnston, S. T., & Eby, M. (2003). Neoproterozoic "snowball Earth": Dynamic sea ice over a quiescent ocean. *Paleoceanography*, *18*(4), n/a-n/a. https://doi.org/10.1029/2003PA000926.

Li, Z.-X., Zhang, L., & McA Powell, C. (1995). *South China in Rodinia: Part of the missing link between Australia-East Antarctica and Laurentia?* Retrieved from https://pubs.geoscienceworld.org/gsa/geology/article-pdf/23/5/407/3515848/i0091-7613-23-5-407.pdf.

McA Powell X Li M W McElhinny, C. Z., Meert, J. G., & Park, J. K. (1993). *Paleomagnetic constraints on timing of the Neoproterozoic breakup of Rodinia and the Cambrian formation of Gondwana*. Retrieved from https://pubs.geoscienceworld.org/gsa/geology/article-pdf/21/10/889/3513943/i0091-7613-21-10-889.pdf.

Park, J. K. (1994). *Palaeomagnetic constraints on the position of Laurentia from middle Neoproterozoic to Early Cambrian times*. Retrieved from https://ac-els-cdn-com.ezproxy.library.wisc.edu/0301926894900817/1-s2.0-0301926894900817-main.pdf?_tid=5b6925e5-84ad-495a-ba26-6c2c2812f723&acdnat=1543591542_dd458438fa27ebeadf071cb539651f3c.

Paul F. Hoffman, Alan J. Kaufman, G. P. H., & Daniel P. Schrag. (1998). A Neoproterozoic Snowball Earth. In *Science* (pp. 1342–1346). https://doi.org/10.1126/science.281.5381.1342

Pierrehumbert, R. T. (2005). Climate dynamics of a hard snowball Earth. *J. Geophys. Res*, *110*, 1111. https://doi.org/10.1029/2004JD005162

Pierrehumbert, R. T., Abbot, D. S., Voigt, A., & Koll, D. (2011). Climate of the Neoproterozoic. *Annual Review of Earth and Planetary Sciences*, *39*(1), 417–460. https://doi.org/10.1146/annurev-earth-040809-152447

Poulsen, C. J., Pierrehumbert, R. T., & Jacob, R. L. (2001). *Impact of ocean dynamics on the simulation of the neoproterozoic "snowball Earth"* (Vol. 28). https://doi.org/10.1029/2000GL012058

Reseaio, G., Lettei•, C. H., & Vol, S. (2001). *CO2 levels required for deglaciation of a "near-snowball" Earth* (Vol. 28). https://doi.org/10.1029/2000GL011836

Rose, B. E. J. (2015). Stable "Waterbelt" climates controlled by tropical ocean heat transport: A nonlinear coupled climate mechanism of relevance to Snowball Earth. *Journal of Geophysical Research*, *120*(4), 1404–1423. https://doi.org/10.1002/2014JD022659

Schopf, J. W., & Klein, C. (1992). *The Proterozoic biosphere : a multidisciplinary study*. Cambridge University Press. Retrieved from https://authors.library.caltech.edu/36446/

Schrag, D. P., Hampt, G., & Murray, D. W. (1996). Pore Fluid Constraints on the Temperature and Oxygen Isotopic Composition of the Glacial Ocean. *Science (New York, N.Y.)*, *272*(5270), 1930–1932. https://doi.org/10.1126/SCIENCE.272.5270.1930

Schrag, D. P., Berner, R. A., Hoffman, P. F., & Halverson, G. P. (2002). On the initiation of a snowball Earth. https://doi.org/10.1029/2001GC000219

Turbet, M., Forget, F., Leconte, J., Charnay, B., & Tobie, G. (2017). CO2 condensation is a serious limit to the deglaciation of Earth-like planets. *Earth and Planetary Science Letters*, *476*, 11–21. https://doi.org/10.1016/J.EPSL.2017.07.050

Tziperman, E., Abbot, D. S., Ashkenazy, Y., Gildor, H., Pollard, D., Schoof, C. G., … Schrag, D. P. (2012). Continental constriction and oceanic ice-cover thickness in a Snowball-Earth scenario. *J. Geophys. Res*, *117*, 5016. https://doi.org/10.1029/2011JC007730

Wang, Y., Huang, B., Dong, Y., Li, S., Zhang, G., & Yu, S. (2018). Geological reconstructions of the East Asian blocks: From the breakup of Rodinia to the assembly of Pangea. *Earth-Science Reviews*, *186*, 262–286. https://doi.org/10.1016/J.EARSCIREV.2018.10.003

Williams, D. M., Kasting, J. F., & Frakes, L. A. (1998). Low-latitude glaciation and rapid changes in the Earth's obliquity explained by obliquity–oblateness feedback. *Nature*, *396*(6710), 453–455. https://doi.org/10.1038/24845.